

MODAL CHARACTERIZATION OF SANDWICH SKEW PLATES

Dhotre PAVAN KUMAR^{*}, Chikkol V. SRINIVASA^{**}

^{*}Research Scholar, Department of Mechanical Engineering, GM Institute of Technology, Davangere, Visvesvaraya Technological University, Jnana Sangama, VTU Main Rd, Machhe, Belagavi, Karnataka 590018, India

^{**}Head, Department of Mechanical Engineering, GM Institute of Technology, Davangere, Visvesvaraya Technological University, Jnana Sangama, VTU Main Rd, Machhe, Belagavi, Karnataka 590018, India

pavankumar-gmitrs@gmit.ac.in, srinivasacv@gmit.ac.in

received 14 March 2021, revised 26 June 2021, accepted 1 July 2021

Abstract: The current work focuses on the experimental and finite element free vibration studies of laminated composite sandwich skew plates. The comparison was made between the experimental values obtained by the Fast Fourier transform (FFT) analyzer and a finite element solution obtained from CQUAD8 finite element of The MacNeal-Schwendler Corporation (MSC) / NASA STRucture Analysis (NAS-TRAN) software. The influence of parameters such as aspect ratio (AR) (a/b), skew angle (α), edge condition, laminate stacking sequence, and fiber orientation angle (θ°) on the natural frequencies of sandwich skew plates was studied. The values obtained by both the finite element and experiment approaches are in good agreement. The natural frequencies increase with an increase in the skew angle for all given ARs.

Keywords: natural frequency, non-dimensional frequency parameter (K_f), antisymmetric laminate, fiber orientation angle, skew angle

1. INTRODUCTION

Due to the reduced weight and high stiffness, sandwich structures have a wide area of applications in engineering science. With anisotropy and considering all parameters involved in the sandwich structure, it is difficult to evaluate the dynamic response analytically. In the literature review, various theories, methods, and techniques were cited (Pavan et al., 2021). However, with the evolution of technology in real engineering applications, it is possible to predict the dynamic response of any structure accurately.

First, an experimental approach to the determination of natural frequencies of sandwich plates was made (Raville et al., 1967). Verification was made (Barkanov et al., 2005) of the numerical results of laminated composite and different sandwich panels with pulse and noncontact laser techniques. Static deformation and free vibration study was conducted on sandwich plates with variable thickness using both numerical and experimental holographic interferometry techniques (Chang et al., 2006). A theoretical and experimental study was conducted on the vibration and acoustical properties of sandwich composite materials (Zhuang, 2006). The vibration testing approach was used to identify the material constants (Lee et al., 2007) and damping characteristics (Berthelot et al., 2008; Maheri et al., 2008; Andena et al., 2012; Petrone et al., 2014; Yang et al., 2014; Abdi et al., 2014) with the help of experimentally obtained natural frequency values of laminated composite sandwich plates. Dynamic behavior of honeycomb sandwich plates was investigated considering the effect of cell size (Adarsh Kumar et al., 2015) and other parameters (Mondal et al., 2015; Rezvani et al., 2018; Prasad et al., 2018; Benjeddou et al., 2019; Arunkumar et al., 2020; Zhicheng et al., 2020) of the honeycomb core. Free vibration and transient dynamic analyses of functionally graded sandwich plates are investigated (Jun Liu et al., 2021) using the scaled boundary finite element method (SBFEM). Nu-

merical studies were presented (Vinayak et al., 2020) on skew composite laminated and sandwich plates under temperature and moisture concentration effects; the laminated sandwich plate is subjected to hygrothermal conditions (Aman et al., 2020) and composite sandwich plates with three-dimensional stress recovery (Su Bin Lee et al., 2020). A review on the analysis of laminated composite and sandwich structures under hygrothermal conditions addressing bending, vibration, buckling, post-buckling, transient, dynamic, and impact studies were made (Aman et al., 2019). An extensive survey on the analysis of sandwich FGM structures under different loading conditions, effects of porosities, hygrothermal loadings, and structures resting on elastic foundations was made (Aman et al., 2020).

A vast amount of literature was reported in detail on free vibration studies for laminated composite skew sandwich plates using analytical and numerical approaches. Limited literature was found related to detailed experimental work on the dynamic response of laminated composite sandwich skew plates. Literature on finite element solutions validated by the experimental method is very scarce. The present paper is an attempt to address this issue in some detail. Fast Fourier transform (FFT) analyzer is an instrument best suited for dynamic applications. In the current work, an FFT analyzer is used for the prediction of natural frequencies of sandwich skew plates.

2. TEST SPECIMEN PREPARATION

The sandwich skew panels were prepared using glass/epoxy laminated composites as face sheets and aluminum honeycomb as core materials. Aluminum honeycomb (Al-3003) panels are

used as the core with a cell size of 6.35 mm, foil thickness of 50 microns, and height of 6 mm. Laminated glass/epoxy reinforced polymer composites are used as face sheets. Unidirectional glass fibers for $[\pm 0^\circ/\text{Core}/\pm 0^\circ]$, $[\pm 90^\circ/\text{Core}/\pm 90^\circ]$ and bidirectional glass fibers for $[\pm 45^\circ/\text{Core}/\pm 45^\circ]$, $[(0^\circ/90^\circ)_s/\text{Core}/(0^\circ/90^\circ)_s]$ of 220 gsm and Lapox L-12 (Epoxy) along with Lapox K-6 hardener were used in fabricating the laminates. Continuous hand lay-up technique was employed for fabricating the sandwich plates, during which the excess resin was removed from the laminate by steel roller. The sandwich laminates are cured at room temperature for a period of 48 h placing weights over them. The test specimens were prepared with fiber weight percentage 50:50 according to relevant American Society for Testing and Materials ASTM standards.

The material constants for aluminum honeycomb core are $E_x = E_y = 0.4043 \text{ MPa}$, $E_z = 941.0802 \text{ MPa}$, $G_{xy} = 0.0546 \text{ MPa}$, $G_{yz} = 110.3007 \text{ MPa}$, $G_{xz} = 73.5338 \text{ MPa}$, $\rho = 48.37 \text{ kg/m}^3$, $\nu_x = 0.994 \approx 1$, and $\nu_y = \nu_z = 0.001$ and evaluated using the formulae presented (Rajkumar S., et al., 2014). ASTM Standard D3039/D3039M (2006) are imposed while evaluating the material properties of laminated glass/epoxy composite panels. The material constants E_1 and E_2 were evaluated experimentally on an average of three trials using Instron Universal Testing Machine at the Central Institute of Plastics Engineering and Technology (CIPET), Mysore, Karnataka, India. Strain gauges were used for calculating strains in longitudinal (along the loading) and transverse (right angles to the loading) directions. The ratio of measured strains concludes the value of Poisson's ratio ν_{12} within the elastic range. The average of three experimental trials was made during the determination of the value of Poisson's ratio ν_{12} . The standard equation of shear modulus presented in Jones(1999) was implemented in calculations and the material properties imposed are given in Tab. 1. The aspect ratio (AR) of the test specimens varied from 1.0 to 2.5 and the skew angle varied from 0° to 45° .

Tab. 1. Material constants of E-glass fiber.

Parameter	Mean	Standard	%Error
E_1 [GPa]	38.07	1.205	0.048
E_2 [GPa]	8.1	0.271	0.033
G_{12} [GPa]	3.05	0.095	0.039
ν_{12}	0.22	0.036	0.015
ρ_{12} [kg/m ³]	2,200		

3. EXPERIMENTAL SETUP

The arrangement for conducting the experimentation is shown in Fig. 1. The test specimen was held in the fixtures, imposing Clamped-Free-Clamped-Free and Clamped-Free-Free-Free edge conditions. A piezoelectric accelerometer sensor was placed at the center of the test specimen using glue and was connected to the FFT analyzer (signal conditioning and amplifying unit). An impact hammer was also connected to the FFT analyzer, dedicated to exciting the test specimen on selected points five times. For each test specimen, five trials were made and an average value was adopted.

Soon, the impact hammer excites the test specimen with a strike (impact); the accelerometer sensor captures the vibration signals and exports them to the FFT analyzer for further pro-

cessing. The FFT analyzer gives the output in terms of Frequency Response Function (FRF) using the pulse lab software. It was ensured that the strike of the impact hammer was normal to the test specimen's surface and no other sources of excitations (surrounding and floor vibrations nearby) were present other than the impact hammer.



Fig. 1. Experimental Setup.

4. FINITE ELEMENT ANALYSIS

MSC/NASTRAN software package was employed for finite element analysis in obtaining the first three fundamental frequencies of skew sandwich plates. Eight-noded isoparametric curved shell elements, i.e., CQUAD8 and CQUAD4, are used in the analysis. A study (Pavan et al., 2020) disclosed that the CQUAD8 element produces more converging and accurate results than the CQUAD4 element. Accordingly, the CQUAD8 element was employed in the present study. To evaluate the real eigenvalues and eigenvectors, the Lanczos method of extraction was imposed for accurate results.

5. RESULTS AND DISCUSSION

The current work focuses on the influence of AR, skew angle, laminate stacking sequence, and edge conditions on the sandwich skew plates. To obtain higher natural frequencies of sandwich skew plates, considering the influence of t_c/t_f and a/h as discussed (Pavan et al., 2021) and minimizing the production cost, twenty-one layer, antisymmetric, angle-ply, and cross-ply laminated sandwich plates are designed and prepared. The thickness ratio of core to face sheet is kept constant in the whole study as $t_c/t_f=6$ and the ratio of length overall thickness a/h is varied to 12.5 ($a/b = 1.0$), 18.75 ($a/b = 1.5$), 25 ($a/b = 2.0$), and 31.25 ($a/b = 2.5$). Two types of edge conditions are implemented in the study i.e., Clamped-Free-Clamped-Free Edge Condition [C-F-C-F] and Clamped-Free-Free-Free Edge Condition [C-F-F-F]. The results from the current study are presented in non-dimensional form using Eq. (1).

$$K_f = 100 \omega a \sqrt{\left(\frac{\rho}{E_1}\right)_f} \tag{1}$$

First, three natural frequencies are extracted from experiments in non-dimensional form. The experimental values are compared with finite element values. The results are tabulated for the C-F-C-F edge condition in Tab. 2 and also graphically presented in Figs. 2–5. The mode shapes are presented in Tab. 3.

The results are tabulated for the C-F-F-F edge condition in Tab. 4 and also graphically presented in Figs. 6–9. The mode shapes are presented in Tab. 5.

Tab. 2. Natural frequencies of Clamped-Free-Clamped-Free laminated composite sandwich skew plates

Mo. No.	Skew Angle (α) 0°							
	Aspect Ratio (alb)							
	1.0		1.5		2.0		2.5	
	Exp	Num	Exp	Num	Exp	Num	Exp	Num
Angle ply $[(+0^\circ/-0^\circ)_s/\text{Core}/(+0^\circ/-0^\circ)_s]$								
1	7.334	7.408	5.539	5.594	4.372	4.415	3.579	3.623
2	9.783	9.892	9.156	9.262	8.759	8.886	8.482	8.628
3	26.069	26.439	22.973	23.283	20.185	20.572	17.862	18.239
Angle ply $[(+45^\circ/-45^\circ)_s/\text{Core}/(+45^\circ/-45^\circ)_s]$								
1	4.945	4.995	3.392	3.425	2.546	2.571	2.026	2.047
2	12.260	12.442	12.273	12.433	12.223	12.403	11.545	11.765
3	20.919	21.301	16.969	17.254	13.826	14.107	12.125	12.377
Angle ply $[(+90^\circ/-90^\circ)_s/\text{Core}/(+90^\circ/-90^\circ)_s]$								
1	4.082	4.123	3.183	3.214	2.139	2.160	1.721	1.738
2	8.569	8.678	8.288	8.390	7.989	8.086	7.837	7.945
3	19.468	19.764	16.398	16.699	12.944	12.376	10.077	10.259
Angle ply $[(0^\circ/90^\circ)_s/\text{Core}/(0^\circ/90^\circ)_s]$								
1	6.278	6.340	4.559	4.604	3.535	3.570	2.874	2.902
2	9.379	9.488	8.817	8.939	8.509	8.611	8.279	8.387
3	24.409	24.813	20.770	21.142	17.800	18.119	15.406	15.667
Skew Angle (α) 15°								
Angle ply $[(+0^\circ/-0^\circ)_s/\text{Core}/(+0^\circ/-0^\circ)_s]$								
1	21.863	22.083	20.491	20.693	18.155	18.338	16.270	16.431
2	23.488	23.777	23.040	23.301	21.665	21.931	20.979	21.226
3	36.405	36.956	41.862	42.451	38.500	39.087	35.901	36.428
Angle ply $[(+45^\circ/-45^\circ)_s/\text{Core}/(+45^\circ/-45^\circ)_s]$								
1	20.018	20.218	17.927	18.105	14.545	14.686	12.410	12.533
2	25.441	25.743	25.188	25.491	24.789	25.098	24.451	24.746
3	40.705	41.355	38.202	38.790	32.905	33.395	29.294	29.800
Angle ply $[(+90^\circ/-90^\circ)_s/\text{Core}/(+90^\circ/-90^\circ)_s]$								
1	18.285	18.461	15.445	15.598	12.193	12.313	10.215	10.315
2	21.183	21.438	20.218	20.463	18.650	18.868	18.013	18.221
3	38.597	39.159	34.982	35.533	29.253	29.663	25.479	25.859
Angle ply $[(0^\circ/90^\circ)_s/\text{Core}/(0^\circ/90^\circ)_s]$								
1	21.085	21.294	19.233	19.423	16.600	16.760	14.528	14.666
2	23.045	23.310	22.585	22.850	21.071	21.311	20.330	20.573
3	42.462	43.088	40.493	41.108	36.461	36.977	33.352	33.837
Skew Angle (α) 30°								
Angle ply $[(+0^\circ/-0^\circ)_s/\text{Core}/(+0^\circ/-0^\circ)_s]$								
1	23.634	23.867	21.080	21.287	18.290	18.470	15.668	15.823
2	25.448	25.747	24.739	25.020	24.381	24.657	24.150	24.440
3	39.264	39.849	43.512	44.141	40.348	40.924	36.453	36.981
Angle ply $[(+45^\circ/-45^\circ)_s/\text{Core}/(+45^\circ/-45^\circ)_s]$								
1	22.285	22.506	19.245	19.437	16.499	16.663	14.212	14.355
2	27.378	27.704	26.379	26.683	25.160	25.447	24.125	24.412
3	44.825	45.273	40.682	41.280	36.629	37.166	32.971	33.445
Angle ply $[(+90^\circ/-90^\circ)_s/\text{Core}/(+90^\circ/-90^\circ)_s]$								
1	20.342	20.545	16.410	16.576	13.315	13.446	11.012	11.122
2	23.465	23.738	22.200	22.459	21.485	21.714	20.930	21.165
3	42.851	43.474	37.288	37.821	32.200	32.680	27.998	28.403
Angle ply $[(0^\circ/90^\circ)_s/\text{Core}/(0^\circ/90^\circ)_s]$								
1	22.945	23.171	19.977	20.173	16.977	17.141	14.480	14.623
2	25.300	25.591	24.673	24.966	24.325	24.600	24.150	24.437
3	43.928	44.590	42.606	43.229	38.342	38.912	34.588	35.121
Skew Angle (α) 45°								
Angle ply $[(+0^\circ/-0^\circ)_s/\text{Core}/(+0^\circ/-0^\circ)_s]$								
1	27.555	27.829	23.435	23.670	19.112	19.300	13.043	13.172
2	29.865	30.221	29.968	30.330	30.210	30.551	26.945	27.262
3	44.752	45.393	47.852	48.553	44.097	44.786	34.248	34.745
Angle ply $[(+45^\circ/-45^\circ)_s/\text{Core}/(+45^\circ/-45^\circ)_s]$								
1	26.785	27.054	23.186	23.419	19.934	20.133	17.786	17.960
2	31.452	31.829	29.254	29.595	27.061	27.369	25.944	26.240
3	49.350	50.058	48.321	49.005	43.598	44.227	41.424	42.022
Angle ply $[(+90^\circ/-90^\circ)_s/\text{Core}/(+90^\circ/-90^\circ)_s]$								
1	24.688	24.930	19.634	19.829	15.678	15.833	16.158	16.319
2	28.255	28.571	27.559	27.862	27.185	27.492	31.001	31.374
3	48.711	49.425	44.562	45.197	38.088	38.638	39.955	40.556
Angle ply $[(0^\circ/90^\circ)_s/\text{Core}/(0^\circ/90^\circ)_s]$								
1	27.008	27.275	22.608	22.829	18.482	18.668	15.679	15.836
2	30.185	30.528	30.589	30.948	30.995	31.348	31.652	32.027
3	48.550	49.241	49.410	50.139	42.975	43.610	39.403	39.977

Tab. 3. Natural frequencies of Clamped-Free-Free-Free laminated composite sandwich skew plates

Mo. No.	Skew Angle (α) 0°							
	Aspect Ratio (alb)							
	1.0		1.5		2.0		2.5	
	Exp	Num	Exp	Num	Exp	Num	Exp	Num
Angle ply $[(+0^\circ/-0^\circ)_s/\text{Core}/(+0^\circ/-0^\circ)_s]$								
1	21.367	21.582	19.878	20.073	18.225	18.400	16.590	16.752
2	22.978	23.247	22.010	22.294	20.965	21.286	19.988	20.370
3	35.461	36.019	40.215	40.887	38.098	38.625	35.568	36.366
Angle ply $[(+45^\circ/-45^\circ)_s/\text{Core}/(+45^\circ/-45^\circ)_s]$								
1	19.336	19.526	16.445	16.609	13.870	14.010	11.789	11.905
2	24.832	25.164	24.810	25.126	24.729	25.042	24.681	24.969
3	39.419	39.997	35.436	36.001	31.550	32.107	28.063	28.530
Angle ply $[(+90^\circ/-90^\circ)_s/\text{Core}/(+90^\circ/-90^\circ)_s]$								
1	17.672	17.848	14.399	14.542	11.868	11.984	9.981	10.081
2	20.500	20.758	18.875	19.090	17.774	18.004	17.115	17.304
3	37.303	37.872	32.580	33.083	28.297	28.756	24.650	25.093
Angle ply $[(0^\circ/90^\circ)_s/\text{Core}/(0^\circ/90^\circ)_s]$								
1	20.728	20.934	18.624	18.810	16.518	16.684	14.631	14.774
2	22.532	22.826	21.249	21.528	20.091	20.339	19.142	19.378
3	41.579	42.210	38.541	39.293	35.829	36.377	33.050	33.537
Skew Angle (α) 15°								
Angle ply $[(+0^\circ/-0^\circ)_s/\text{Core}/(+0^\circ/-0^\circ)_s]$								
1	21.863	22.083	20.491	20.693	18.155	18.338	16.270	16.431
2	23.488	23.777	23.040	23.301	21.665	21.931	20.979	21.226
3	36.405	36.956	41.862	42.451	38.500	39.087	35.901	36.428
Angle ply $[(+45^\circ/-45^\circ)_s/\text{Core}/(+45^\circ/-45^\circ)_s]$								
1	20.018	20.218	17.927	18.105	14.545	14.686	12.410	12.533
2	25.441	25.743	25.188	25.491	24.789	25.098	24.451	24.746
3	40.705	41.355	38.202	38.790	32.905	33.395	29.294	29.800
Angle ply $[(+90^\circ/-90^\circ)_s/\text{Core}/(+90^\circ/-90^\circ)_s]$								
1	18.285	18.461	15.445	15.598	12.193	12.313	10.215	10.315
2	21.183	21.438	20.218	20.463	18.650	18.868	18.013	18.221
3	38.597	39.159	34.982	35.533	29.253	29.663	25.479	25.859
Angle ply $[(0^\circ/90^\circ)_s/\text{Core}/(0^\circ/90^\circ)_s]$								
1	21.085	21.294	19.233	19.423	16.600	16.760	14.528	14.666
2	23.045	23.310	22.585	22.850	21.071	21.311	20.330	20.573
3	42.462	43.088	40.493	41.108	36.461	36.977	33.352	33.837
Skew Angle (α) 30°								
Angle ply $[(+0^\circ/-0^\circ)_s/\text{Core}/(+0^\circ/-0^\circ)_s]$								
1	23.634	23.867	21.080	21.287	18.290	18.470	15.668	15.823
2	25.448	25.747	24.739	25.020	24.381	24.657	24.150	24.440
3	39.264	39.849	43.512	44.141	40.348	40.924	36.453	36.981
Angle ply $[(+45^\circ/-45^\circ)_s/\text{Core}/(+45^\circ/-45^\circ)_s]$								
1	22.285	22.506	19.245	19.437	16.499	16.663	14.212	14.355
2	27.378	27.704	26.379	26.683	25.160	25.447	24.125	24.412
3	44.825	45.273	40.682	41.280	36.629	37.166	32.971	33.445
Angle ply $[(+90^\circ/-90^\circ)_s/\text{Core}/(+90^\circ/-90^\circ)_s]$								
1	20.342	20.545	16.410	16.576	13.315	13.446	11.012	11.122
2	23.465	23.738	22.200	22.459	21.485	21.714	20.930	21.165
3	42.851	43.474	37.288	37.821	32.200	32.680	27.998	28.403
Angle ply $[(0^\circ/90^\circ)_s/\text{Core}/(0^\circ/90^\circ)_s]$								
1	22.945	23.171	19.977	20.173	16.977	17.141	14.480	14.623
2	25.300	25.591	24.673	24.966	24.325	24.600	24.150	24.437
3	43.928	44.590	42.606	43.229	38.342	38.912	34.588	35.121
Skew Angle (α) 45°								
Angle ply $[(+0^\circ/-0^\circ)_s/\text{Core}/(+0^\circ/-0^\circ)_s]$								
1	27.555	27.829	23.435	23.670	19.112	19.300	13.043	13.172
2	29.865	30.221	29.968	30.330	30.210	30.551	26.945	27.262
3	44.752	45.393	47.852	48.553	44.097	44.786	34.248	34.745
Angle ply $[(+45^\circ/-45^\circ)_s/\text{Core}/(+45^\circ/-45^\circ)_s]$								
1	26.785	27.054	23.186	23.419	19.934	20.133	17.786	17.960
2	31.452	31.829	29.254					

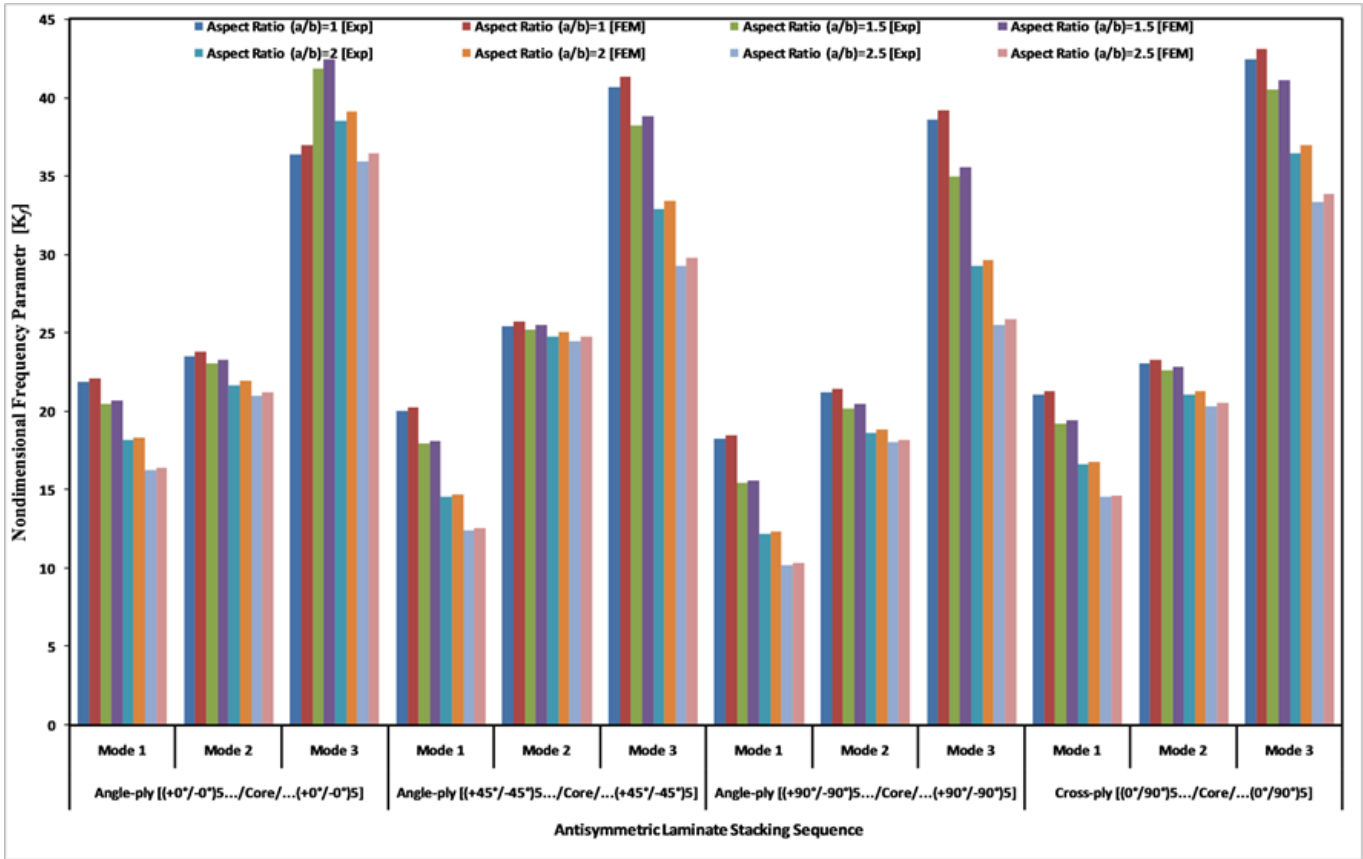


Fig. 2. Variation of K_f with AR (a/b) for C-F-C laminated composite sandwich skew plates with skew angle $\alpha = 0^\circ$.

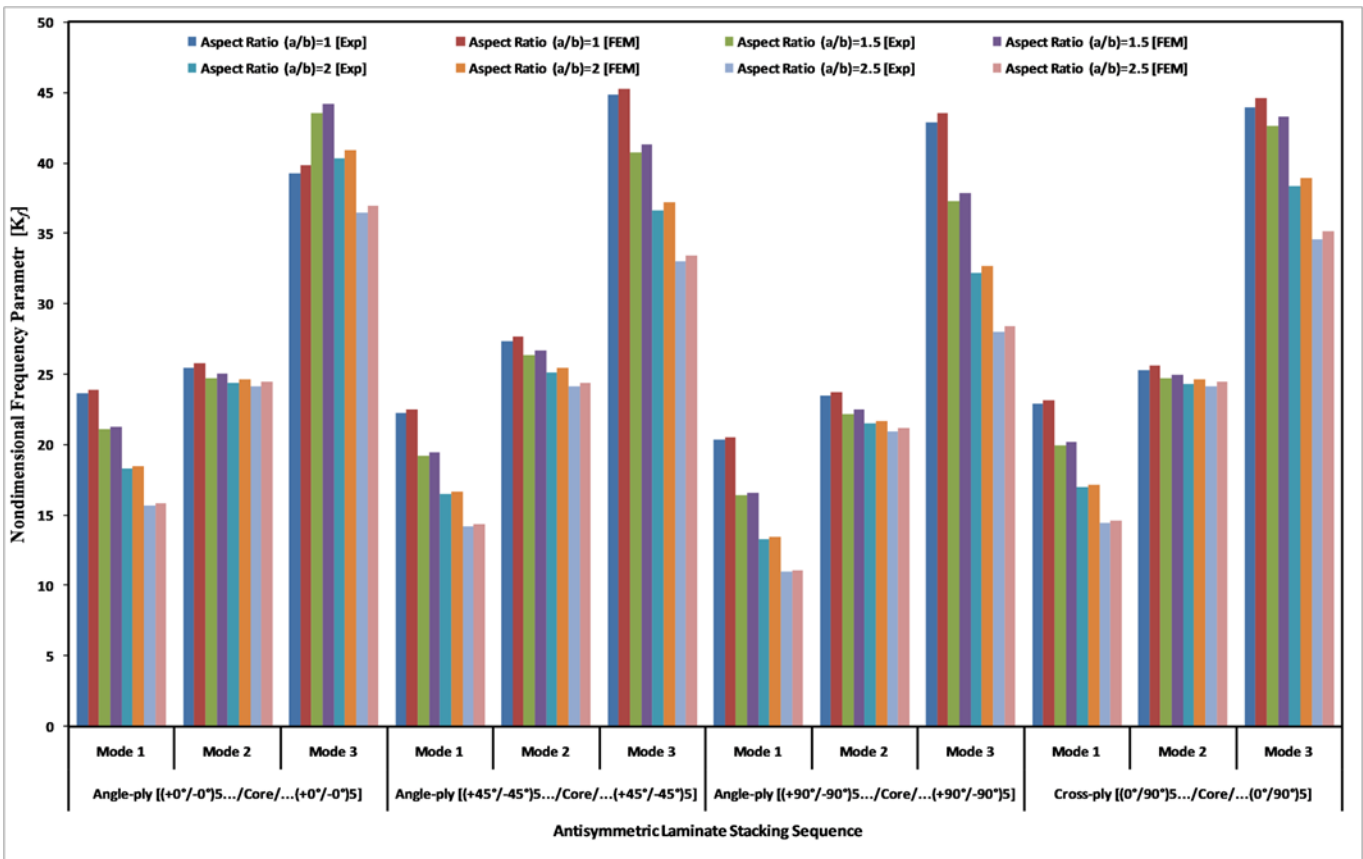


Fig. 3. Variation of K_f with AR (a/b) for C-F-C laminated composite sandwich skew plates with skew angle $\alpha = 15^\circ$.

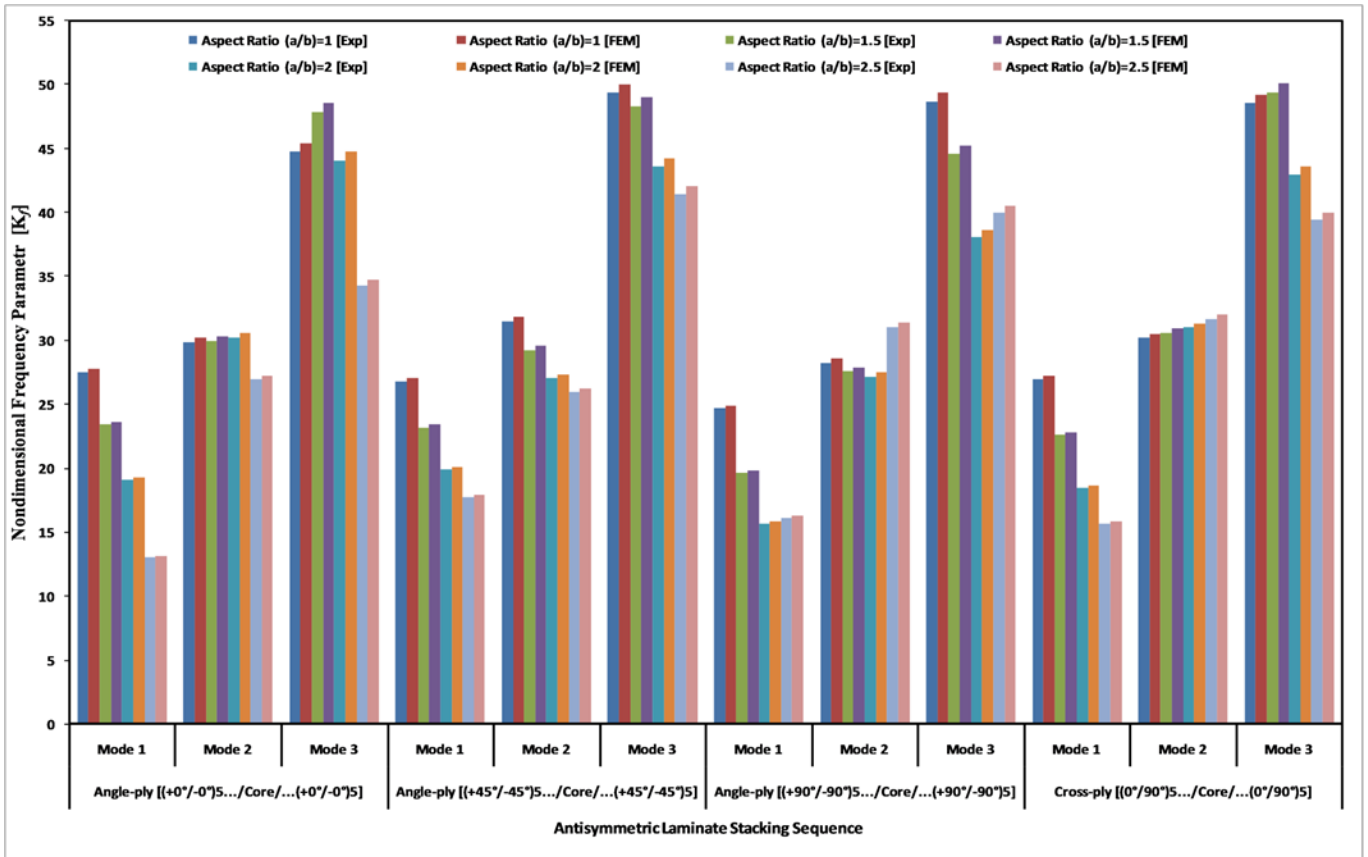


Fig. 4. Variation of K_f with AR (a/b) for C-F-C-F laminated composite sandwich skew plates with skew angle $\alpha = 30^\circ$.

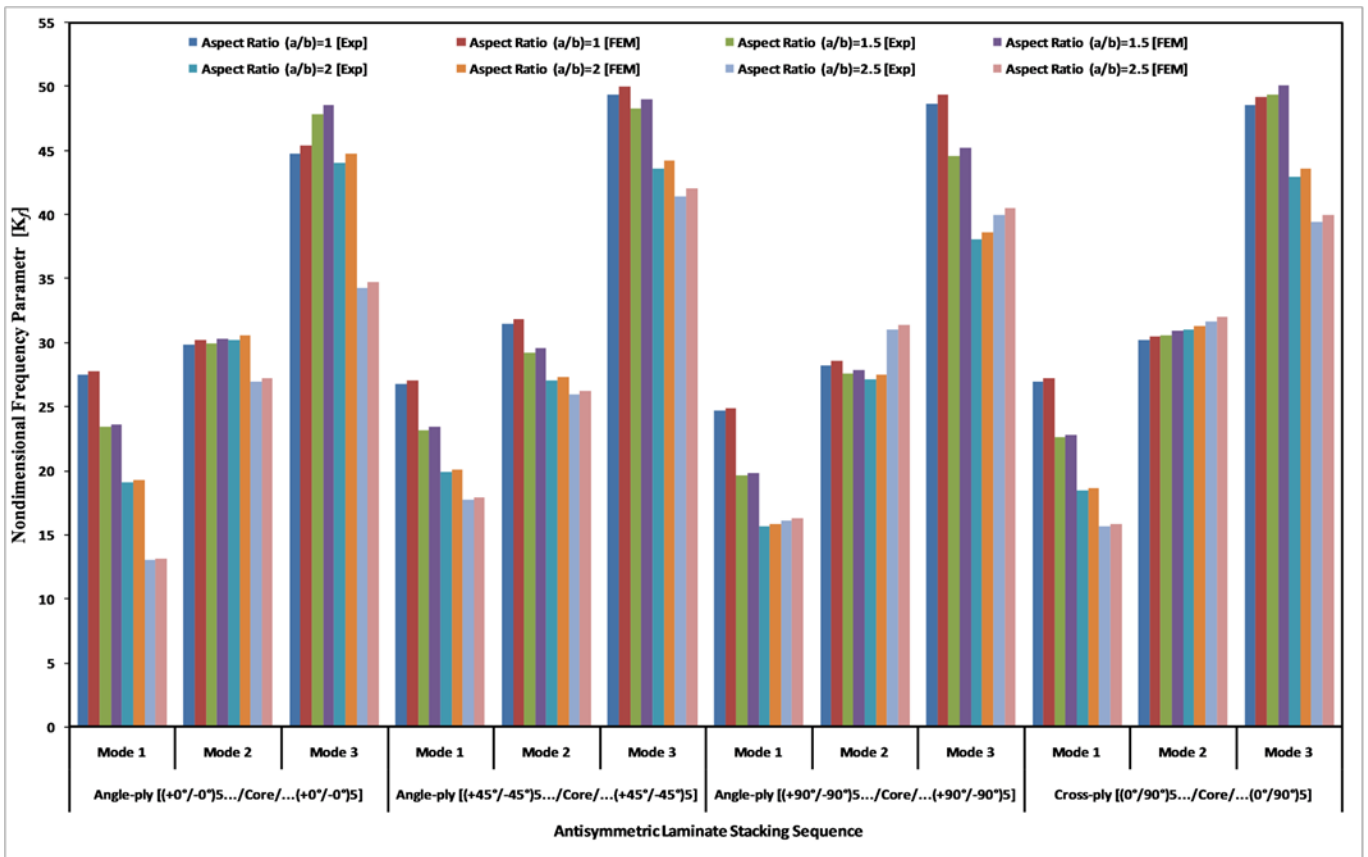


Fig. 5. Variation of K_f with AR (a/b) for C-F-C-F laminated composite sandwich skew plates with skew angle $\alpha = 45^\circ$.

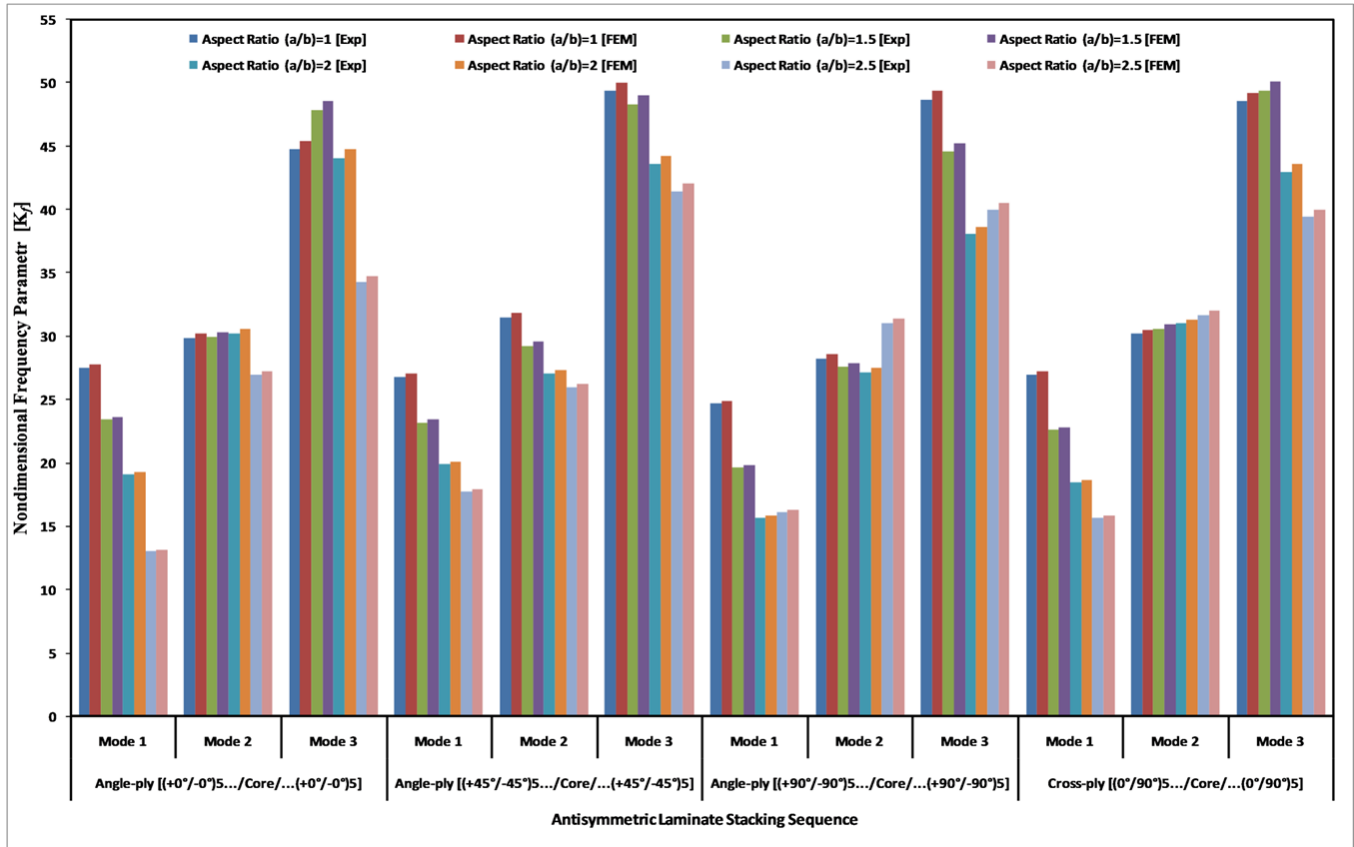


Fig. 6. Variation of K_f with AR (a/b) for C-F-F laminated composite sandwich skew plates with skew angle $\alpha = 0^\circ$.

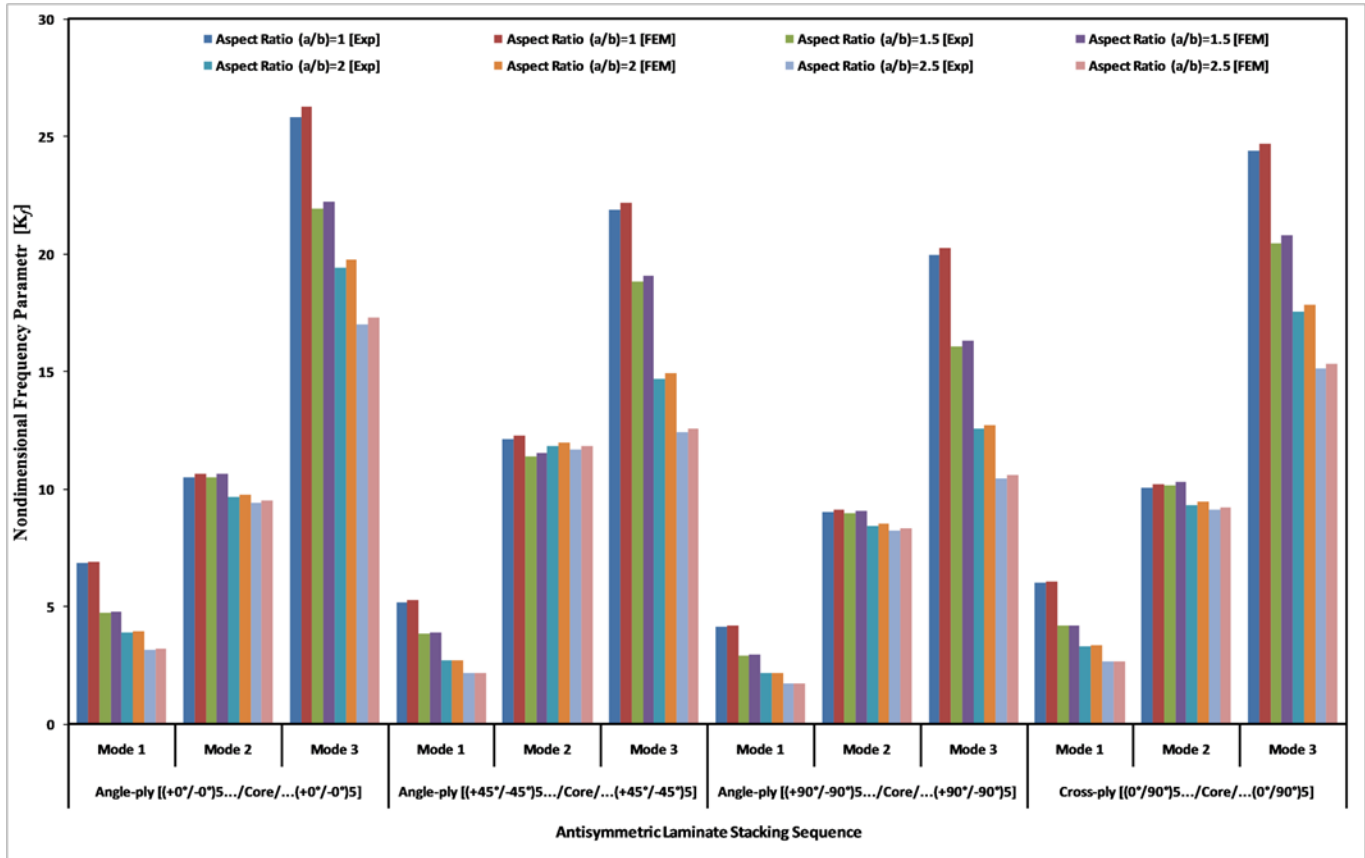


Fig. 7. Variation of K_f with AR (a/b) for C-F-F laminated composite sandwich skew plates with skew angle $\alpha = 15^\circ$.

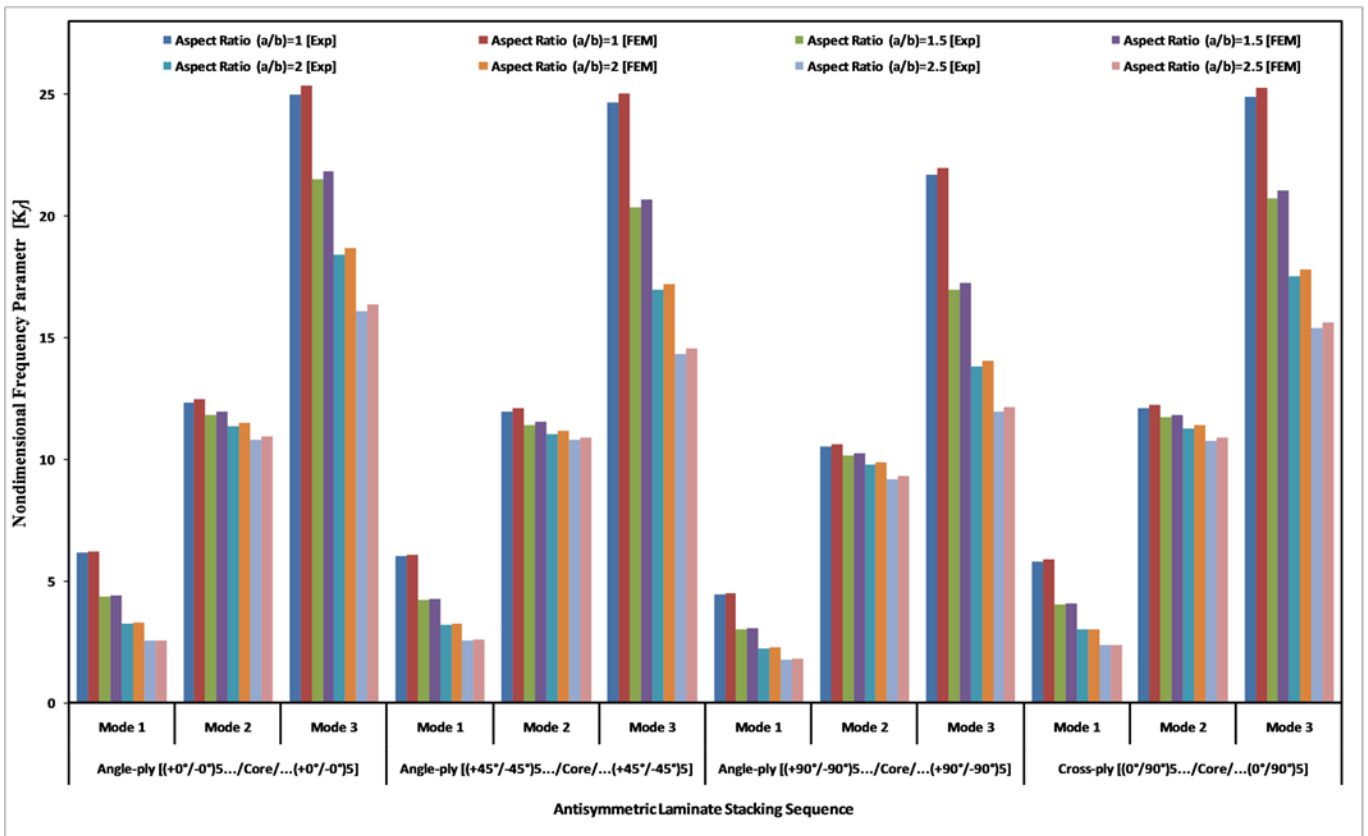


Fig. 8. Variation of K_f with AR (a/b) for C-F-F-F laminated composite sandwich skew plates with skew angle $\alpha = 30^\circ$.

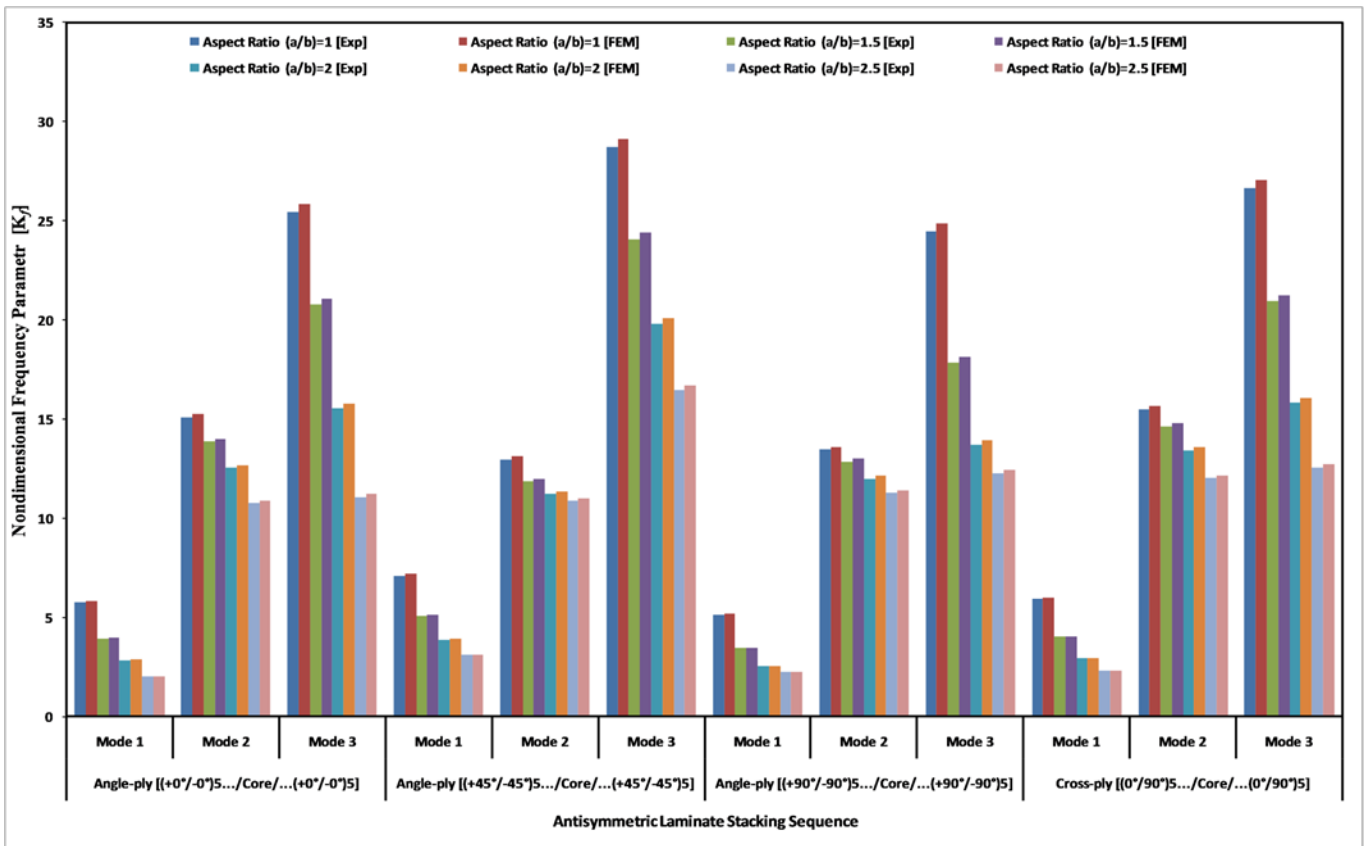
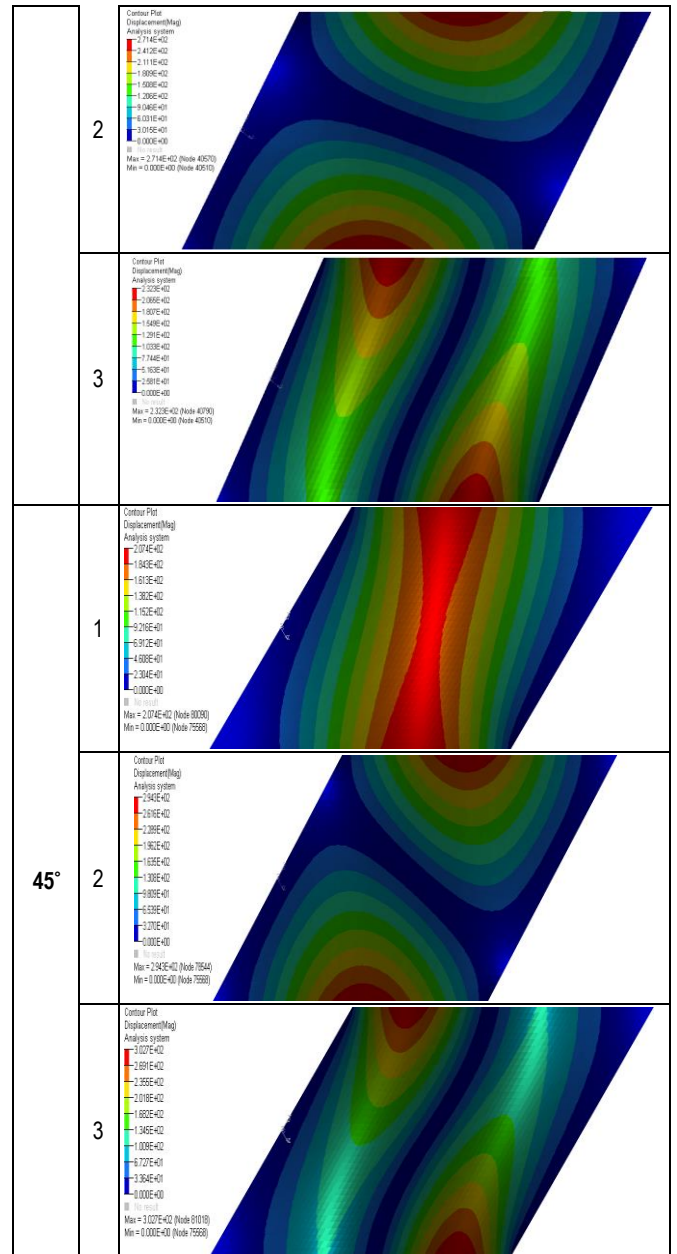


Fig. 9. Variation of K_f with AR (a/b) for C-F-F-F laminated composite sandwich skew plates with skew angle $\alpha = 45^\circ$.

Tab. 4. Mode shapes for C-F-C-F laminated composite sandwich skew plates ($a/b = 1.5$, $NL = 21$, antisymmetric cross-ply laminate)

Skew Angle	Mode Shapes [NL=21 AR=1.5]	
0°	1	
	2	
	3	
15°	1	
	2	
	3	
30°	1	



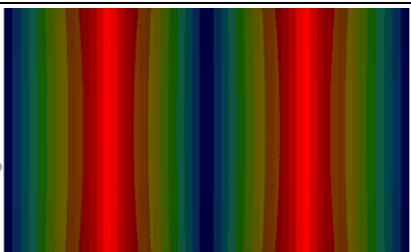
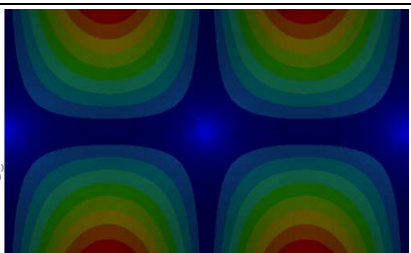
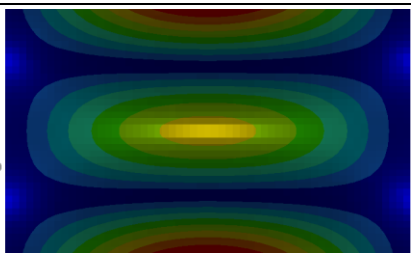
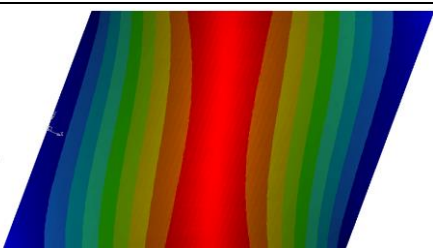
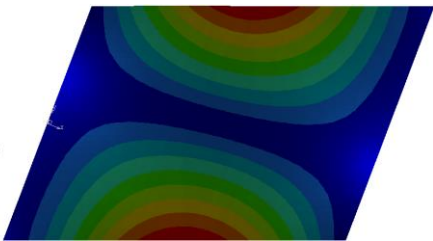
Figs. 2–5 clearly explain that:

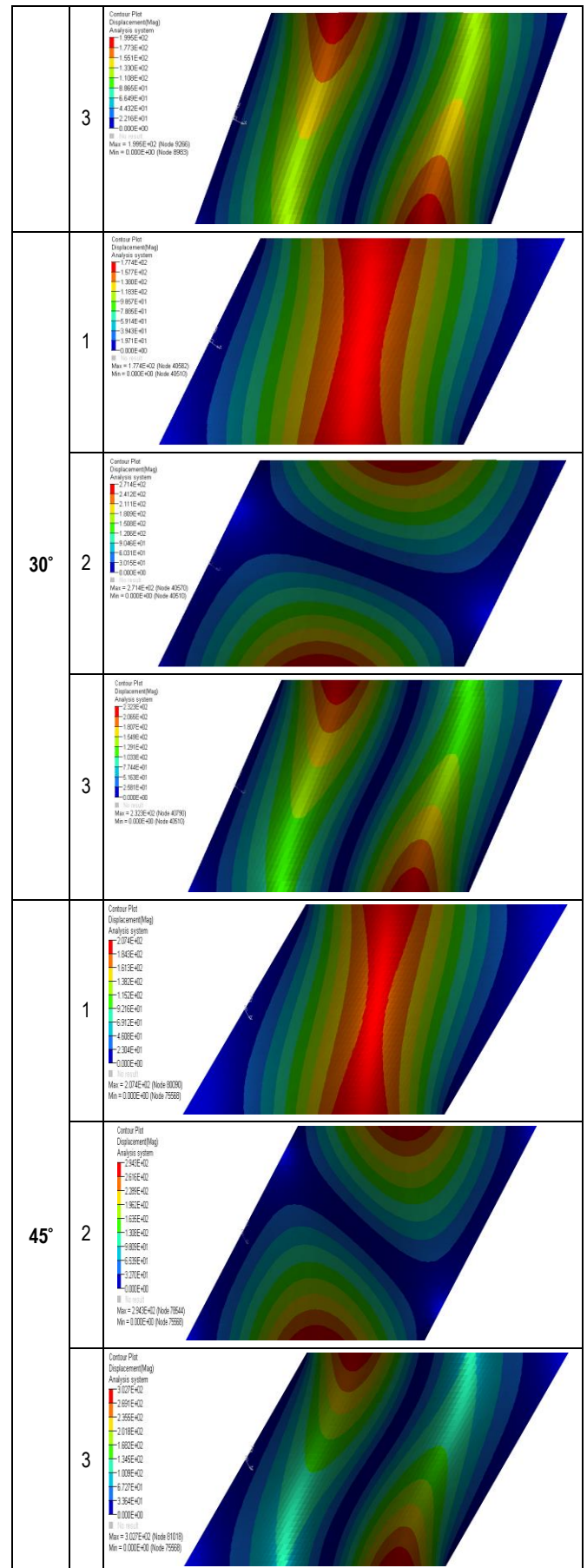
- For laminate stacking sequence angle ply $[(\pm 0^\circ)_5/\text{Core}/(\pm 0^\circ)_5]$, the first natural frequency decrease with an increase in the AR. AR is the ratio of length to width, where width is kept constant and only length is varied. As the AR increases, the length of the plate increases, which makes the plate less stiff, leading to a decrease in the natural frequency. For the second natural frequency, it decreases with an increase in AR except for skew = 45°. For skew 0° to 45°, as the skew angle increases, the width of the plate decreases due to the skew, and also the overall area of the plate goes on reducing. This makes the plate lighter and at the same time stiffer. For the third natural frequency, it increases from AR = 1 to AR = 1.5, then it decreases, it is due to the combined effect of fiber orientation, mode shape, mass density, and stiffness of the plate.
- For angle ply $[(\pm 45^\circ)_5/\text{Core}/(\pm 45^\circ)_5]$ the first and third natural frequencies decrease with an increase in the AR for a given skew angle. However, in the second natural frequency, variation is negligible for skew = 0°; it is considerable for other

skew angles. Here the plate produces more stiffness due to the fiber orientation and it overshadows the effect of plate stiffness due to the change in the AR compared to other skew angles.

- In angle ply $[(\pm 90^\circ)_s/\text{Core}/(\pm 90^\circ)_s]$ stacking sequence, for all three frequencies, the K_f value decreases as the increase in the AR except skew = 45° . For skew = 45° the K_f value decreases from AR = 1 to AR = 1.5 and then it increases. It is exactly opposite as in the case of angle ply $[(\pm 0^\circ)_s/\text{Core}/(\pm 0^\circ)_s]$.
- The K_f value decreases with an increase in the AR in all the three modes of cross-ply $[(0^\circ/90^\circ)_s/\text{Core}/(0^\circ/90^\circ)_s]$ stacking sequence from skew = 0° to 30° . The only exception is for skew = 45° in which the second natural frequency goes on increasing as the AR increased. The third natural frequency first increases from AR = 1 to AR = 1.5 and then decreases.

Tab. 5. Mode shapes for C-F-F laminated composite sandwich skew plates ($a/b = 1.5$, $NL = 21$, antisymmetric cross-ply laminate)

Skew Angle	Mode Shapes [NL=21, AR=1.5]
0°	<p>1</p> 
	<p>2</p> 
	<p>3</p> 
15°	<p>1</p> 
	<p>2</p> 



And from Figs. 6–9, the following is observed:



- With skew = 15° for cross-ply $[(0^\circ/90^\circ)_5/\text{Core}/(0^\circ/90^\circ)_5]$ and Angle ply $[(\pm 45^\circ)_5/\text{Core}/(\pm 45^\circ)_5]$, the second natural frequency decreases then it increases and it increases then it decreases is the only change.
- The K_f value decreases in the order of laminate stacking sequence: angle ply $[(\pm 0^\circ)_5/\text{Core}/(\pm 0^\circ)_5]$, cross-ply $[(0^\circ/90^\circ)_5/\text{Core}/(0^\circ/90^\circ)_5]$, angle ply $[(\pm 45^\circ)_5/\text{Core}/(\pm 45^\circ)_5]$ angle ply $[(\pm 90^\circ)_5/\text{Core}/(\pm 90^\circ)_5]$.
- For a given value of AR, as the skew angle is increased, the value of K_f increases considerably (Pavan K., et al., 2021).
- The values of K_f are higher for C-F-C-F than C-F-F-F edge conditions for any given AR and skew angle.
- The experimental values in the form of the non-dimensional frequency coefficient K_f are very close to accurate and promising to those of the finite element solution.

6. CONCLUSION

Free vibration investigation was made on laminated sandwich skew plates adopting both experimental and finite element methods. Glass epoxy laminated composites are used as face sheets and aluminum honeycomb (Al3003) is used as the core in the current study. Two types of edge conditions were used. i.e., C-F-C-F and C-F-F-F. The experimentally obtained results were then validated by finite element values, and the experimental values are promising and close to the finite element values. Influences of various parameters, for instance, skew angle, AR, laminate stacking sequence, and edge conditions are studied. The thickness ratio of core to face sheet $t_c/t_f = 6$ was kept constant all through the study. As the AR increases for any skew angle, the K_f value decreases irrespective of the edge condition. When the AR increases, the length of the sandwich plate also increases. This reduces the stiffness of the sandwich skew plate. The skew angle plays a major role in the dynamic response of the sandwich skew plate. When the skew angle is increased, the K_f value increases for all ARs. The fiber orientation of the lamina plays a significant role in deciding the vibration response of the sandwich skew plates. When the fiber angle is 0° i.e., the fiber is placed parallel to the length of the plate, the plate produces higher natural frequency due to more stiffness in the longitudinal direction. In addition, the lowest natural frequency is observed when the fiber angle is 90° i.e., the fiber angle is perpendicular to the length of the plate. The natural frequencies for the other laminate stacking sequences lie in between these two extreme values. The sandwich skew plates with C-F-C-F edge conditions produce a higher natural frequency than plates with C-F-F-F edge conditions.

REFERENCES

1. **Abdi B., Azwan S., Ayob A., Rahman R.A., Abdullah R.A.** (2014), Experimental Investigation on Free Vibration of Foam-Core Sandwich Plate with and without Circular Polymer Columns, *Advanced Materials Research*, 845, 297-301.
2. **Adarsh K., Ramesh S.S.** (2015), Modal Analysis and Testing of Honeycomb Sandwich Composites, Topics in Modal Analysis, Volume 10, *Proceedings of the 33rd IMAC, A Conference and Exposition on Structural Dynamics*, Springer International Publishing, 237-241.
3. **Aman G., Chalak H.D.** (2019), A review on analysis of laminated composite and sandwich structures under hygrothermal conditions, *Thin-Walled Structures*, 142, <https://doi.org/10.1016/j.tws.2019.05.005>.
4. **Aman G., Chalak H.D.** (2020), Analysis of non-skew and skew laminated composite and sandwich plates under hygro-thermo mechanical conditions including transverse stress variations, *Journal of Sandwich Structures and Materials*, DOI: 10.1177/1099636220932782.
5. **Aman G., Mohamed O.B., Chalak H.D., Anupam C.** (2020), A review of the analysis of sandwich FGM structures, *Composite Structures*, <https://doi.org/10.1016/j.compstruct.2020.113427>.
6. **Andena L., Manconi E., Manzoni S., Moschini S., Vanali M.** (2012), Experimental tests and numerical modeling of a sandwich panel, *25th International Conference on Noise and Vibration engineering (ISMA2012), 4th International Conference on Uncertainty in Structural Dynamics (USD2012), Leuven*.
7. **Arun Kumar M.P., Jeyaraj P., Ganga Dharan K.V., Surya Narayana Reddy C.V.** (2020), Numerical and experimental study on dynamic characteristics of honeycomb core sandwich panel from equivalent 2D model, *Sadhana*, 45, 206, 1-6.
8. **Barkanov E., Chate A., Skukis E., Täger O., Kolsters H.** (2005), Finite element and experimental vibration analysis of viscoelastic composite structures, *Computational Methods and Experimental Measurements XII*, 41, 527-537.
9. **Benjeddou A., Guerich M.** (2019), Free vibration of actual aircraft and spacecraft hexagonal honeycomb sandwich panels: A practical detailed FE approach, *Advances in Aircraft and Spacecraft Science*, 6(2), 169-187.
10. **Berthelot J.M., Assarar M., Sefrani Y., Mahi A.E.** (2008), Damping analysis of composite materials and structures, *Composite Structures*, 85, 189-204.
11. **Chang J.S., Chen H.C., Lin H.T.** (2006), Numerical and experimental studies on aluminum sandwich plates of variable thickness, *Journal of the Chinese Institute of Engineers*, 29(5), 851-862.
12. **Jones R.M.** (1999), *Mechanics of Composite Materials*, Taylor and Francis.
13. **Jun L., Congkuan H., Wenbin Y., Fan Y., Gao L.** (2021), Free vibration and transient dynamic response of functionally graded sandwich plates with power-law nonhomogeneity by the scaled boundary finite element method, *Computer Methods in Applied Mechanics and Engineering*, 376, <https://doi.org/10.1016/j.cma.2021.113665>.
14. **Lee C.R., Kam T.Y., Sun S.J.** (2007), Free-Vibration Analysis and Material Constants Identification of Laminated Composite Sandwich Plates, *Journal of Engineering Mechanics*, 133 (8), 874-886.
15. **Maheri M.R., Adams R.D., Hugon J.** (2008), Vibration damping in sandwich panels, *Journal of Material Science*, 43, 6604-6618.
16. **Mondal S., Patra A.K., Chakraborty S., Mitra N.** (2015), Dynamic performance of sandwich composite plates with circular hole/cut-out: A mixed experimental-numerical study, *Composite Structures*, 131, 479-489.
17. **Pavan K., Srinivasa C.V.** (2020), Free vibration studies on skew sandwich plates by FEM, *IOP Conference Series: Materials Science and Engineering*, 925, 012024, Doi:10.1088/1757-899X/925/1/012024.
18. **Pavan K., Srinivasa C.V.** (2020), On buckling and free vibration studies of sandwich plates and cylindrical shells: A review, *Journal of thermoplastic composite materials*, 33 (5), 1-51.
19. **Pavan K.D., Srinivasa C.V.** (2021), On free vibration of laminated skew sandwich plates: A Finite element analysis, *Nonlinear Engineering*, <https://doi.org/10.1515/nleng-2021-0006>, 2021.
20. **Petrone G., Alessandro V.D., Franco F., Mace B., De Rosa S.** (2014), Modal characterisation of recyclable foam sandwich panels, *Composite Structures*, 113, 362-368.
21. **Prasad E.V., Sahu S.K.** (2018), Vibration Analysis of Woven Fiber Metal Laminated Plates — Experimental and Numerical Studies,

- International Journal of Structural Stability and Dynamics*, 18, 1850144-1-23.
22. **Rajkumar S., Ravindran D., Ramesh S.S., Raghupathy V.P.** (2014), Evaluation of elastic constants of A3003 honeycomb core with varying hexagonal cell geometries through finite element approach, *Proceedings of the Institution of Mechanical Engineers Part C Journal of Mechanical Engineering Science*, 203-210, DOI: 10.1177/0954406213510491.
 23. **Raville M.E., Ueng C.E.S.** (1967), Determination of Natural Frequencies of Vibration of a Sandwich Plate, *Experimental Mechanics*, 7, 490-493, <https://doi.org/10.1007/BF02326265>.
 24. **Rezvani S.S., Kiasat M.S.** (2018), Analytical and experimental investigation on the free vibration of a floating composite sandwich plate having viscoelastic core, *Archives of Civil and Mechanical Engineering*, 18, 1241-1258.
 25. **Su Bin L., Chang-Yong L., Dewey H.H.** (2020), On the mechanics of composite sandwich plates with three-dimensional stress recovery, *International Journal of Engineering Science*, 157.
 26. **Vinayak K., Balaji K., Kattimani S.C.** (2020), Effect of temperature and moisture on free vibration characteristics of skew laminated hybrid composite and sandwich plates, *Thin-Walled Structures*, 157, <https://doi.org/10.1016/j.tws.2020.107113>.
 27. **Yang J.S., Xiong J., Ma L., Wu L.Z.** (2014), Vibration and damping performances of carbon fiber composite pyramidal truss sandwich panels embedded with viscoelastic layers, *ECCM16 - 16TH European conference on composite materials*, Seville, Spain, 22-26.
 28. **Zhicheng H., Xingguo W., Nanxing W., Fulei C., Jing L.** (2020), The Finite Element Modeling and Experimental Study of Sandwich Plates with Frequency-Dependent Viscoelastic Material Model, *Materials*, 13, 2296, Doi:10.3390/ma13102296.
 29. **Zhuang L.** (2006), *Vibration and acoustical properties of sandwich composite*, Degree of Doctor of Philosophy, Auburn University, Auburn, Alabama.
- Acknowledgments: The authors would like to express gratitude to the Principal and Management of GM Institute of Technology, India, for their inspiration and support provided.
- Dhotre Pavan Kumar:  <https://orcid.org/0000-0002-7900-755X>
- Chikkol V. Srinivasa:  <https://orcid.org/0000-0002-9794-3886>